Rev. Adv. Mater. Sci. 50 (2017) 37-46

SPLIT DISLOCATION LOOPS AND JOGGED DISLOCATIONS IN DEFORMED COLUMNAR-GRAINED NANOTWINNED METALS

I.A. Ovid'ko and A.G. Sheinerman[1,2,3]

[1]Research Laboratory for Mechanics of New Nanomaterials, Peter the Great St. Petersburg Polytechnic University, St. Petersburg 195251, Russia
[2]Institute of Problems of Mechanical Engineering, Russian Academy of Sciences, St. Petersburg 199178, Russia
[3]St. Petersburg State University, St. Petersburg 198504, Russia

Received: November 21, 2016

Abstract. A theoretical model is suggested which describes two plastic deformation mechanisms in deformed columnar-grained nanotwinned metals loaded parallel to coherent twin boundaries. The first mechanism represents the formation and expansion of split dislocation loops within individual twins, while the second one assumes the emission of split jogged dislocations from grain boundaries into grain interiors. Within the model, both split dislocation loops and jogged dislocations are generated at pre-existent full dislocations at grain boundaries. Under these assumptions, the critical stresses for the nucleation and expansion/motion of split dislocation loops and jogged dislocations are calculated. It is demonstrated that at a specified grain size, the critical stress for the formation and motion of jogged dislocations is always smaller than that for the expansion of split dislocation loops across twin lamellae. The results explain the inconsistencies of molecular dynamics simulation results [H. Zhou et al., *Nano Lett.* **14** (2014) 5075; Y. Zhu et al., *Int. J. Plasticity* **72** (2015) 168] concerning the possibility for the coexistence of split dislocation loops and jogged dislocations in nanotwinned metals and multilayers.

1. INTRODUCTION

Due to their superior mechanical properties, including ultrahigh strength, good tensile ductility and superb fatigue resistance, and excellent electric conductivity, nanotwinned metals have attracted considerable interest during last decade (see, e.g., reviews [1–8] and original articles [9–21]). Among various nanotwinned structures one can distinguish columnar–grained nanotwinned metals. Such metals have pronounced {111} out-of-plane texture, and their coherent twin boundaries (CTBs) are primarily located normally to the axes of cylindrical grains (e.g., [21–24]). Due to the presence of pronounced texture, columnar-grained nanotwinned metals possess high plastic anisotropy, and their plastic deformation mechanisms depend dramatically on the orientation(s) of the applied load. When the applied load is directed parallel to CTBs, the plastic deformation mechanisms acting in untextured nanotwinned metals – dislocation glide from one CTB to another as well as dislocation motion along CTBs – are largely suppressed. In this case, molecular dynamics (MD) simulations suggest the following two dominant plastic deformation mechanisms in columnar-grained metals: formation and expansion

Corresponding author: A.G. Sheinerman, e-mail: asheinerman@gmail.com

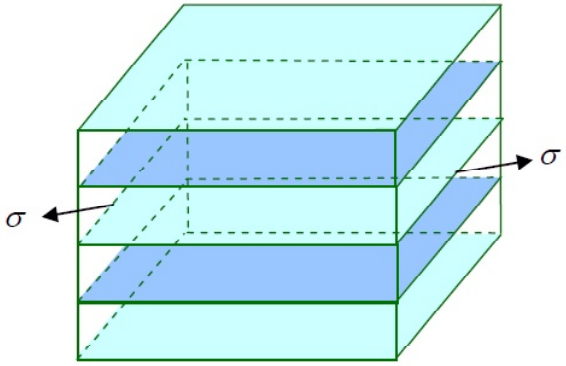

Fig. 1. A fragment of nanotwinned solid loaded parallel to CTBs.

of split dislocation loops [22,23,25,26] (that consist of threading segments spanning individual twins and "misfit" segments that lie in CTBs) and the motion of split jogged, necklace-like dislocations that thread multiple twin planes [25,26]. The authors of MD simulations [25] observed the transition from the first deformation mechanism (the formation of dislocation loops within individual twins) to the second one (the formation and motion of jogged dislocations) as the twin thickness decreased below 1 nm and suggested that the combined action of these deformation mechanisms is possible only in a narrow twin thickness range where the critical stresses for the activation of these mechanisms are approximately the same. At the same time, MD simulations [26] of Cu/Ag nanotwinned multilayered films demonstrated the combined action of these deformation mechanisms. Also, the simple theoretical estimates of the critical stresses for the activation of both mechanisms made in paper [25] suggest that at small twin thickness, the critical (minimum) stress for the expansion of split dislocation loops within individual twins is smaller than that for the motion of jogged dislocation. This estimate is in direct contradiction with the observation of jogged dislocations (not accompanied by any individual dislocation loops) at ultrasmall twin thickness in the same paper. Thus, the conditions for the actions of different deformation mechanisms in columnar-grained nanotwinned metals need further investigation. The aim of this paper is to suggest a theoretical model describing the deformation mechanisms in columnar-grained metals (loaded parallel to CTBs) through the formation of split dislocation loops and jogged dislocations and to calculate the critical stresses for the activation of these deformation mechanisms.

2. GENERATION OF A SPLIT DISLOCATION LOOP FROM A GRAIN BOUNDARY OF A NANOTWINNED METAL

Consider a columnar-grained nanotwinned metallic specimen with a face-centered cubic (fcc) crystal lattice. Such a specimen consists of columnar grains that comprise parallel twins divided by parallel coherent twin boundaries (CTBs). Let a uniaxial tensile load σ be applied parallel to the CTBs (Fig. 1). Within our model, grain boundaries (GBs) of the specimen are approximated as planes. We assume that a full lattice dislocation has been formed at a GB of the nanotwinned specimen before its deformation. Also, we suppose that under the action of the applied tensile load σ, plastic deformation in a grain occurs either via the nucleation and expansion of a split dislocation loop within a specified twin (Figa. 2a and 2b) or through the emission of a split jogged dislocation that threads the entire grain (Figs. 2c and 2d). Both the split dislocation loop and the split jogged dislocation are supposed to nucleate at the pre-existing dislocation at a GB and glide under the action of the resolved shear stress created in the CTB planes by the applied load σ.

First, examine the formation of a split dislocation loop at the pre-existent dislocation at a GB (Fig. 3). Such a process occurs through the formation and expansion of a leading Shockley dislocation loop followed by the generation and expansion of a trailing Shockley dislocation loop. For convenience, we assume that the GB is normal to the CTBs and model the dislocation loops as rectangular ones (Fig. 3). Since dislocations in fcc solids glide along the <110> directions in the {111} planes, we define the direction of the dislocation glide as $[\bar{1}10]$. Then the pre-existent dislocation occupies the direction $[\bar{1}\bar{1}2]$ (Fig. 3). Next, we define the Burgers vectors of the pre-existent full dislocation, leading dislocation loop and trailing dislocation loop as $\mathbf{b}_0$, $\mathbf{b}_1$, and $\mathbf{b}_2$, respectively. For definiteness, we define the Burgers vectors $\mathbf{b}_1$ and $\mathbf{b}_2$ as follows: $\mathbf{b}_1 = (a/6)[\bar{2}11]$ and $\mathbf{b}_2 = (a/6)[\bar{1}\bar{1}2]$, where a is the crystal lattice parameter. Then the sum Burgers vector $\mathbf{b}_1 + \mathbf{b}_2$ of the split dislocation loop is $\mathbf{b}_1 + \mathbf{b}_2 = (a/2)[\bar{1}01]$. Also, we denote the twin thickness as d and introduce the Cartesian coordinate system as shown in Fig. 3. For simplicity, we further assume that the Burgers vector $\mathbf{b}_0$- $\mathbf{b}_1$- $\mathbf{b}_2$ lies in the plane (x,y) and denote the projection of the Burgers vector $\mathbf{b}_0$ onto the (x,y) plane as $\mathbf{b}_{||}$, the angle between the vector $\mathbf{b}_{||}$ and the x-axis as δ

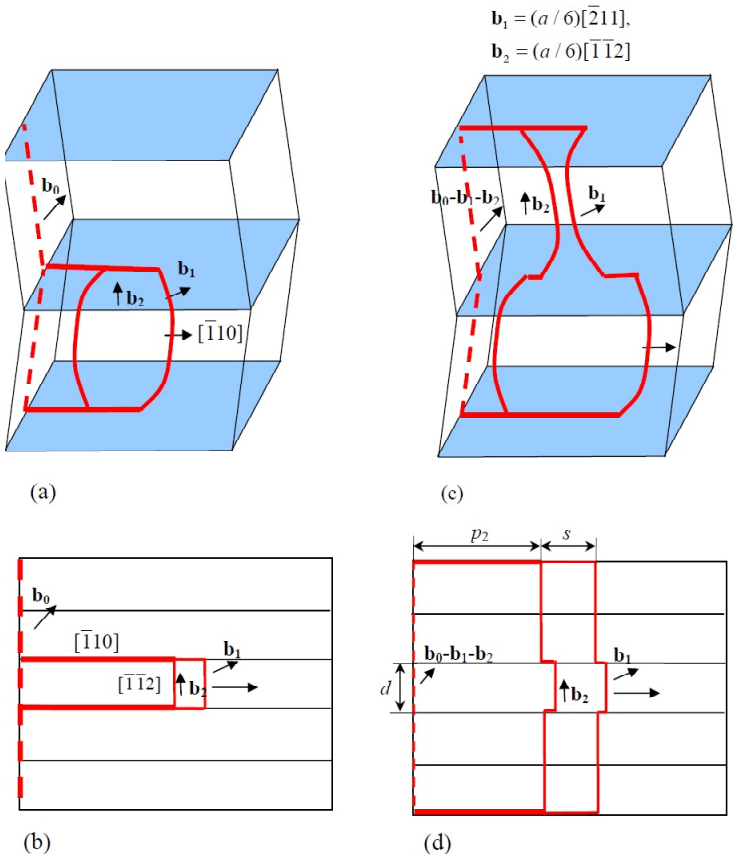

Fig. 2. Split dislocation loop (a,b) and jogged dislocation (c,d) in a columnar-grained nanotwinned solid. (a,c) Dislocation configurations in MD simulations [25,26]. (b,d) Dislocation configurations in our model.

(Fig. 3c), and the angle between the dislocation loop slip plane (111) and the CTB plane as φ (φ=arccos(1/3)≈70.5°). Finally, we designate and the angle between the direction of the applied load σ and the *x*-axis as β (Fig. 3d).

Since the formation of a split dislocation loop requires the formation of a leading dislocation loop, first, examine the latter process (Fig. 3a). We designate the specific energy of the stacking fault produced in the flat region inside the loop as γ and denote the sizes of the loop in the direction of the *x*-axis as p_1. For simplicity, we focus on the situation where the loop quickly grows along the *z*-axis until its maximum length *d* and then starts to expand along the *x*-axis (Fig. 3a). To estimate the conditions for the formation of the loop with the dimensions p_1 and *d*, we calculate the energy ΔW_1 associated with its formation. The energy ΔW_1 can be presented as

$$\Delta W_1 = W_1^s + W_{d-1}^{\text{int}} - A_1^\sigma + W_1^c + \Delta W_{d1}^c + W_1^\gamma - W_{CTB}, \quad (1)$$

where W_1^s is the proper strain energy of the leading dislocation loop, W_{d-1}^{int} is the energy of its elastic interaction with the pre-existent dislocation at the GB, A_1^σ is the work of the applied stress s on the loop expansion, W_1^c is the energy of the loop core, ΔW_{d1}^c is the change of the core energy of the initial dislocation due to the loop formation, W_1^γ is the energy of the stacking fault, and W_{CTB} is the energy of the CTB fragments removed by the upper and lower loop sides AB and CD (Fig. 3a).

In the approximation of an elastically isotropic solid with the shear modulus *G* and Poisson's ratio ν, the proper strain energy of the leading dislocation loop is given [27,28] by $W_1^s = Db^2 g_1^s$, where $D=G/[2\pi(1-\nu)]$,

$$g_1^s = (2-\nu)(h_1 - p_1 - d) + (1-\nu\sin^2\alpha_1) d \ln\frac{2p_1 d}{r_0(h_1+d)} + (1-\nu\cos^2\alpha_1) p_1 \ln\frac{2p_1 d}{r_0(h_1+p_1)}, \quad (2)$$

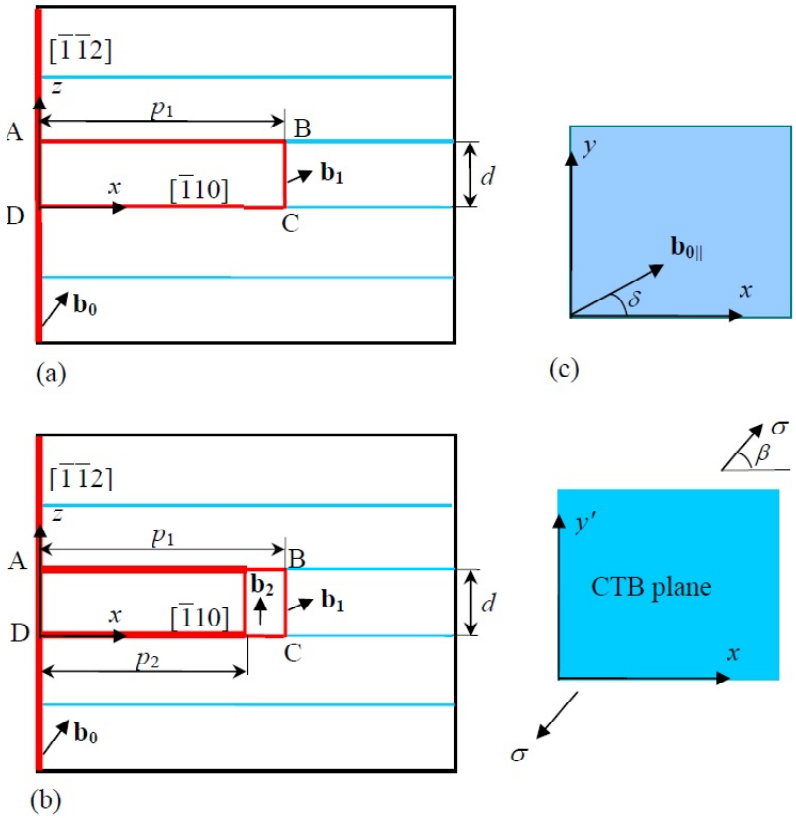

Fig. 3. Geometry of a partial dislocation loop (a) and split dislocation loop (b) in a deformed nanotwinned metal. Figures (c) and (d) illustrate the orientation of the Burgers vector $\mathbf{b}_0$ of the pre-existent dislocation and the direction of the applied load σ, respectively.

$h_1 = \sqrt{d^2 + p_1^2}$, α_1=π/6, b=$a/\sqrt{6}$ is the magnitude of the Burgers vector $\mathbf{b}_1$, and r_0=$a/\sqrt{2}$ is the interatomic distance.

The energy W_{d-1}^{int} of the elastic interaction of the leading dislocation loop with the pre-existent dislocation at the GB is calculated as

$$W_{d-1}^{\text{int}} = -d\int_{r_0}^{p_1} [b_{1x}\sigma_{xy}^{d}(x, y=0) + b_{1z}\sigma_{yz}^{d}(x, y=0)]\,dx, \qquad (3)$$

where $\sigma_{xy}^{d}(x,y)$ is the component of the stress field of the initial dislocation. From the expressions [29] for the stress field of straight dislocations in an isotropic infinite medium, we have: $\sigma_{xy}^{d}(x,y=0)=Db_{0x}/x = Db_0\cos\delta/(2x)$ (where b_0=$a/\sqrt{2}$ is the magnitude of the Burgers vector $\mathbf{b}_0$) and $\sigma_{zy}^{d}(x,y=0)=(1-\nu)Db_{0z}/x = Db_0\sqrt{3}/(2x)$. Substitution of the latter relations to formula (3) yields

$$W_{d-1}^{\text{int}} = -\frac{3Db^2 d}{4}\ln\frac{p_1}{r_0}(1-\nu+\cos\delta). \qquad (4)$$

The work A_1^{σ} of the applied stress σ on the loop expansion can be calculated as

$$A_1^{\sigma} = (b_{1x}\sigma_{xy'} + b_{1y'}\sigma_{y'y'})\,p_1 d\sin\varphi, \qquad (5)$$

where $\sigma_{xy'}$ and $\sigma_{y'y'}$ are the components of the stress created by the applied load σ in the coordinate system (x,y') shown in Fig. 3d. Since $\sigma_{xy'}$= σcosβsinβ, $\sigma_{y'y'}$=sin²β, φ=arccos(1/3), $b_{1y'}$=b_{1z}cosφ=b/6 and b_{1x}=$b\sqrt{3}$/2, one can rewrite formula (5) in the form

$$A_1^{\sigma} = \sigma bd\,p_1\left(\frac{\sqrt{6}}{6}\sin(2\beta) + \frac{\sqrt{2}}{9}\sin^2\beta\right). \qquad (6)$$

The core energy W_1^c of the three new dislocation segments AB, BC, and CD formed due to the loop formation is calculated in a standard way from the expressions [29] for the core energies of edge and screw dislocations as

$$W_1^c = \frac{(4-\nu)Db^2(2p_1+d)}{8}. \qquad (7)$$

The change ΔW_{d1}^c of the core energy of the segment AD of the initial dislocation due to the loop formation (associated with a change of the Burgers vector of this dislocation segment from $\mathbf{b}_0$ to $\mathbf{b}_0$- $\mathbf{b}_1$) is obtained in a similar way as

$$\Delta W_{d1}^c = -\frac{Db^2 d}{8}(2-5\nu+6\cos\delta). \tag{8}$$

The energy of the stacking fault is given by $W_1^\gamma = \gamma p_1 d$. Finally, the energy W_{CTB} of the CTB fragments removed by the upper and lower loop sides AB and CD is given by $W_{CTB}=2\gamma_{CTB} p_1 r_0$, where γ_{CTB} is the specific CTB energy. The latter relations and formulae (1), (2), (4), and (6)–(8) give the expressions for the energy ΔW_1. Now the critical stress σ_{c1} that represents the minimum value of the applied load for the loop generation can be obtained from the relation $\Delta W_1(p_1 = p')|_{\sigma=\sigma_{c1}} = 0$, where p' is a parameter. For definiteness, we put $p'=2r_0$.

The dependences of the critical stress σ_{c1} on the parameter δ are plotted in Fig. 4 for $\beta=\pi/3$, various values of the twin thickness d and the case of Cu characterized by the following parameter values: G=48 GPa, ν=0.34, a=0.361 nm, γ=47 mJ/m^2 and γ_{CTB}=24 mJ/m^2. If σ_{c1}<0, in Fig. 4 we put σ_{c1}=0. Fig. 4 clearly demonstrates that σ_{c1} weakly depends on d, and at δ smaller than around 50°, the generation of the first dislocation loop is always favorable. The generation of the dislocation loop is unlikely only for unflavored orientations of the initial dislocation Burgers vector characterized by the values of δ exceeding 50 to 60 degrees.

If the first dislocation loop nucleates, it expands until it has reached its equilibrium dimensions. The expansion of the leading dislocation loop is hindered by the high energies of stacking faults. At the same time, the generation and expansion of the first dislocation loop can be followed by the generation of a trailing dislocation loop and subsequent simultaneous expansion of the two loops in the form of a split dislocation loop (Fig. 3b). To analyze the generation and expansion of a split dislocation loop, let us calculate the energy ΔW associated with its formation. To do so, we denote the size of the trailing dislocation loop in the direction of the x-axis as p_2. The energy ΔW can be presented in the following form:

$$\begin{aligned}\Delta W &= W_1^s + W_2^s + W_{1-2}^{\text{int}} + W_{d-1}^{\text{int}} + W_{d-2}^{\text{int}} \\ &- A_1^\sigma - A_2^\sigma + W_{12}^c + \Delta W_d^c + W^\gamma - W_{CTB}.\end{aligned} \tag{9}$$

In formula (9), W_2^s is the proper strain energy of the trailing dislocation loop, W_{d-2}^{int} is the energy of its elastic interaction with the pre-existent dislocation at the GB, W_{1-2}^{int} is the energy of the elastic interaction between the leading and trailing dislocation loop, A_2^σ is the work of the applied stress σ on the trailing dislocation loop expansion, W_{12}^c is the total energy of the loop cores, ΔW_d^c is the change of the core energy of the initial dislocation at the GB due to the formation of two dislocation loops, W^γ is the energy of the stacking fault, and the other terms are defined as above.

The proper strain energy of the trailing dislocation loop is given [27,28] by $W_2^s = Db^2 g_2^s$, where

$$\begin{aligned}g_2^s &= (2-\nu)(h_2 - p_2 - d) \\ &+(1-\nu\sin^2\alpha_2)d\ln\frac{2p_2 d}{r_0(h_2+d)} \\ &+(1-\nu\cos^2\alpha_2)p_2\ln\frac{2p_2 d}{r_0(h_2+p_2)},\end{aligned} \tag{10}$$

$h_2 = \sqrt{d^2+p_2^2}$ and $\alpha_2=\pi/2$.

The energy of the elastic interaction between the leading and the trailing dislocation loop is given [28] by $W_{1-2}^{\text{int}} = Db^2 g_{1-2}^{\text{int}}$, where

$$\begin{aligned}g_{1-2}^{\text{int}} &= (2-\nu)\cos(\alpha_1-\alpha_2) \\ &\times(h_1+h_2-S-d-2p_2) \\ &+ d[\cos(\alpha_1-\alpha_2)-\nu\sin\alpha_1\sin\alpha_2] \\ &\times\ln\frac{2dp_1p_2(d+S)}{r_0(p_1-p_2)(d+h_1)(d+h_2)} \\ &+[\cos(\alpha_1-\alpha_2)-\nu\cos\alpha_1\cos\alpha_2] \\ &\times\left(p_1\ln\frac{p_1(p_1-p_2+S)}{(p_1-p_2)(p_1+h_1)}+\right. \\ &\left.p_2\ln\frac{4d^2(p_1-p_2)p_2}{r_0^2(p_1-p_2+S)(p_2+h_2)}\right)\end{aligned} \tag{11}$$

and $S=\sqrt{d^2+(p_1-p_2)^2}$.

The energy W_{d-2}^{int} of the elastic interaction of the trailing dislocation loop with the pre-existent dislocation at the GB is calculated in the same fashion as the energy W_{d-1}^{int} and follows as

$$W_{d-2}^{\text{int}} = -\frac{3(1-\nu)Db^2 d}{2}\ln\frac{p_2}{r_0}. \tag{12}$$

The work A_2^σ of the applied stress σ on the loop expansion is calculated in the same way as the work A_1^σ and presented as

$$A_2^\sigma = \frac{2\sqrt{2}}{9}\sin^2\beta\,\sigma b d p_2. \tag{13}$$

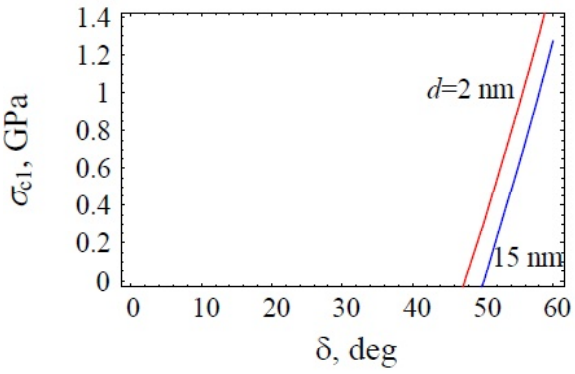

Fig. 4. Dependences of the critical stress σ_{c1} for the generation of a partial dislocation loop within a twin on the angle δ characterizing the orientation of the Burgers vector $\mathbf{b}_0$ of the pre-existent dislocation, for different values of twin thickness d.

The total core energy W_{12}^c of the new dislocation segments AB, BC, and CD formed due to the formation of two dislocation loops is calculated in a standard way from the expressions [29] for the core energies of edge and screw dislocations as

$$W_{12}^c = \frac{Db^2}{8}[2(4-3\nu)(p_1+2p_2)+d(8-7\nu)]. \quad (14)$$

The change ΔW_d^c of the core energy of the segment AD of the initial dislocation due to the formation of two dislocation loops (and associated with a change of the Burgers vector of this dislocation segment from $\mathbf{b}_0$ to $\mathbf{b}_0$- $\mathbf{b}_1$- $\mathbf{b}_2$) is obtained in a similar way as

$$\Delta W_d^c = -\frac{Db^2 d}{8}(10-9\nu+2\cos\delta). \quad (15)$$

The energy of the stacking fault is given by $W^{\gamma}=\gamma(p_1-p_2)d$.

Now the energy ΔW is given by the latter relation and formulae (2), (4), (6), and (9)–(15). The contour maps of the energy ΔW in the coordinate space (p_1,p_2) are shown in Fig. 5 for the case of nanotwinned Cu with d=40 nm, $\beta=\pi/3$, $\delta=\pi/12$ and various values of the applied load σ. Fig. 5a demonstrates that at relatively small values of σ (σ =0.6 GPa), after the expansion of the leading dislocation loop, the trailing dislocation loop has to overcome some energetic barrier to nucleate until its size p_2 along the x-axis has reached around 0.5 nm. After that, the simultaneous expansion of the leading and trailing dislocation loop (that is, the motion of the split dislocation loop) becomes energetically beneficial until the loops have reached their equilibrium

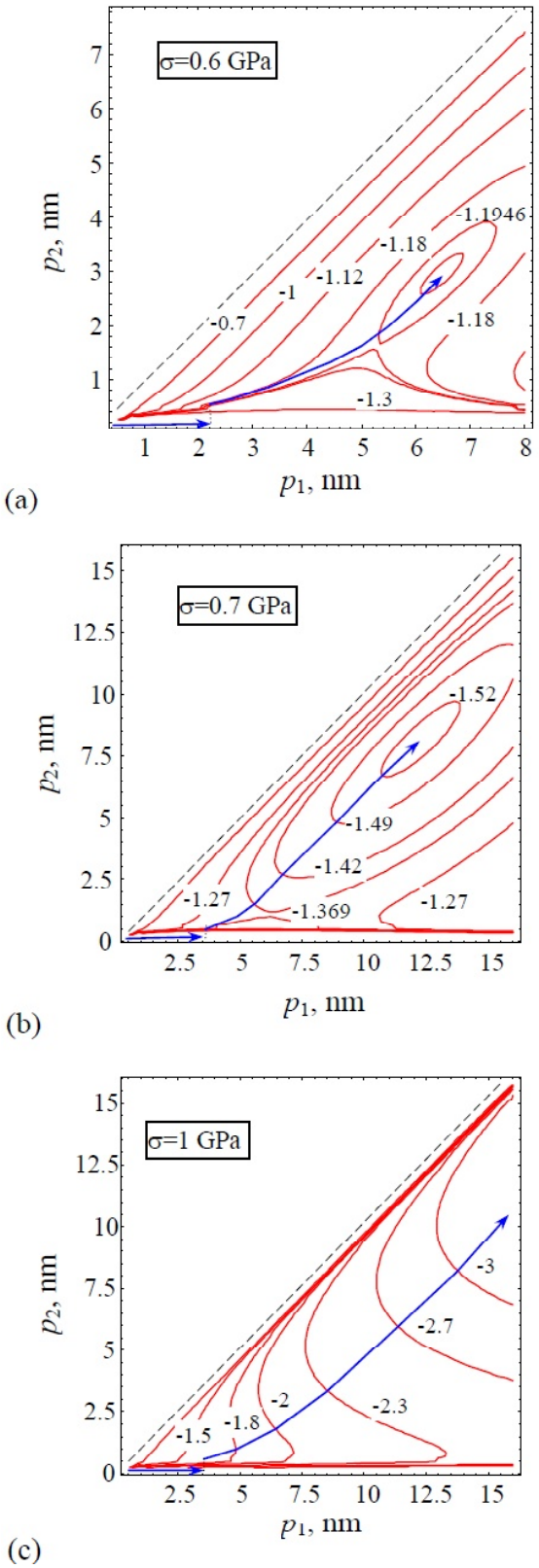

Fig. 5. Contour maps of the energy ΔW associated with the formation of a split dislocation loop within a twin in the coordinate space (p_1,p_2). The energy ΔW is given in units of 10^{-17} J. The blue arrows show the growth trajectory of the split dislocation loop corresponding to the maximum energy gradient, and their ends in figures (a) and (b) correspond to the equilibrium loop dimensions.

sizes $p_1 \approx 6.5$ nm and $p_2 \approx 3$ nm. Fig. 5b shows that at a larger value of the applied load ($\sigma = 0.7$ GPa), the equilibrium sizes of the loops increase up to $p_1 \approx 12$ nm and $p_2 \approx 8$ nm. With further increase in σ, the equilibrium sizes of the loops further increase until the expansion of the split dislocation loop across the entire twin becomes energetically beneficial (Fig. 5c). The latter situation takes place when the value of the applied load σ exceeds some critical stress σ_c^∞. The critical stress σ_c^∞ is calculated from the condition that at $\sigma > \sigma_c^\infty$, the energy ΔW should decrease with the characteristic distance p_2 from the GB to the split dislocation at large values of p_2. Thus, the relation for σ_c^∞ has the following form: $\lim_{p_2 \to \infty} (\partial \Delta W(p_1 = p_2 + s, \sigma = \sigma_c^\infty) / \partial p_2) = 0$, where s is the distance between the vertical segments of the leading and threading dislocation loop. Substitution of the expressions for the energy ΔW to the latter relation yields

$$\sigma_c^\infty = \frac{3Db^2[(4-\nu)\ln(d/r_0) + 4 - 3\nu] - 4\sqrt{2}\,a\gamma_{CTB}}{8\sqrt{2}\,bd\sin\beta\cos(\beta - \pi/6)}. \quad (16)$$

The dependence $\sigma_c^\infty(d)$ is plotted in Fig. 6 for the case of nanotwinned Cu with $\beta = \pi/3$. Fig. 6 demonstrates that σ_c^∞ decreases with increasing d. Also, for $d < 40$ nm, $\sigma_c^\infty > 1$ GPa. This means that at small values of twin thickness, the critical stress σ_c^∞ is very high, and the formation of split dislocation loops requires very high applied stresses. Therefore, in the next section we consider the conditions for the action of another mechanism of plastic deformation in columnar-grained nanotwinned metals loaded parallel to CTBs, namely, the formation of split jogged dislocations.

3. GENERATION OF A SPLIT JOGGED DISLOCATION AT A GRAIN BOUNDARY OF A NANOTWINNED METAL

Now consider the emission of a split jogged dislocation by a GB containing a pre-existent dislocation with the Burgers vector $\mathbf{b}_0$. The split jogged dislocation is assumed to consist of the leading and trailing Shockley partial dislocations (with the Burgers vectors $\mathbf{b}_1$ and $\mathbf{b}_2$, respectively) joined by a stacking fault. The emission of the above dislocations from the pre-existent dislocation changes its Burgers vector from $\mathbf{b}_0$ to $\mathbf{b}_0$-$\mathbf{b}_1$-$\mathbf{b}_2$ (Figs. 2c and 2d). The Burgers vectors $\mathbf{b}_0$, $\mathbf{b}_1$ and $\mathbf{b}_2$ are defined as

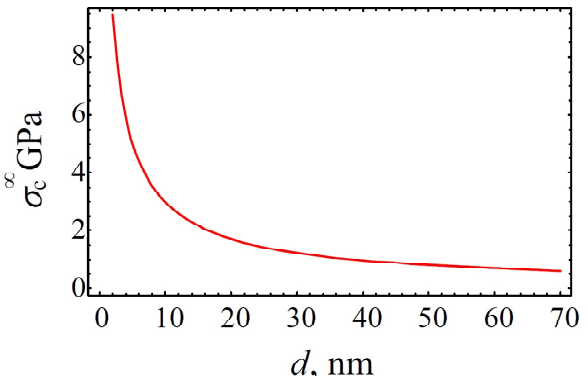

Fig. 6. Dependence of the critical stress σ_c^∞ for the expansion of the split dislocation loop through the entire twin on twin thickness d.

above. Also, following the results of molecular dynamics (MD) simulations [25,26], jogged dislocation produce nanoscale kinks at the CTBs. Therefore, as a first approximation, we model the jogged dislocations as straight dislocations containing kinks at the CTBs (Fig. 2d). The motion of the leading and trailing jogged dislocations is supposed to occur through the consecutive motion of their segments located within individual twins, accompanied by the formation of paired kinks that bound these segments (Fig. 2d). Also, we denote the distance from the GB to the trailing dislocation as p_2, and the distance between the leading and trailing dislocation as s (Fig. 2d).

To estimate the critical stresses for the formation of split jogged dislocations, we calculate the forces acting on the segments of the leading and trailing dislocations located within an individual twin (Fig. 2d). The projections F_{1x} and F_{2x} of the force acting on the segment (of length d) of the leading and trailing dislocation, respectively, onto the x-axis can be presented as

$$F_{1x} = F_1^\sigma - \gamma d + F_1^{pin} + F_{2-1}^{\text{int}} + F_{d-1}, \quad (17)$$

$$F_{2x} = F_2^\sigma + \gamma d + F_2^{pin} + F_{1-2}^{\text{int}} + F_{d-2}. \quad (18)$$

In formulae (17) and (18), F_1^σ and F_2^σ are the projections (onto the x-axis) of the forces exerted on the segments of the leading and trailing dislocation, respectively, by the applied load σ, the second terms represent the forces exerted by the stacking fault, F_1^{pin} and F_2^{pin} are the projections of the forces associated with the formation of kink pairs, $F_{2\text{-}1}$ is the projection of the force exerted by the trailing dislocation on the leading one, $F_{1\text{-}2}$ is the projection

of the force exerted by the leading dislocation on the trailing one, and $F_{d\text{-}1}$ and $F_{d\text{-}2}$ are the forces exerted on the leading and trailing dislocation, respectively, by the residual dislocation with the Burgers vector $\mathbf{b}_0$- $\mathbf{b}_1$-$\mathbf{b}_2$, situated at the GB.

The forces F_1^σ and F_2^σ are calculated in the same fashion as the works A_1^σ and A_2^σ and can be written as

$$F_1^\sigma = \sigma bd\left(\frac{\sqrt{6}}{6}\sin(2\beta)+\frac{\sqrt{2}}{9}\sin^2\beta\right),$$
$$F_2^\sigma = \frac{2\sqrt{2}}{9}\sin^2\beta\,\sigma bd. \qquad (19)$$

The forces F_1^{pin} and F_2^{pin} are assumed to be associated with the core energies of the paired kinks and are as follows: $F_1^{pin} = -Db^2(1\text{-}3\nu/4)$, $F_2^{pin} = -Db^2$. The forces $F_{1\text{-}2}$ and $F_{2\text{-}1}$ of the interaction between the segments of the leading and trailing dislocations are given by the standard formula [29]: $F_{2\text{-}1}=-F_{1\text{-}2} = Db^2(1\text{-}\nu)d/(2s)$. Similarly, the forces $F_{d\text{-}1}$ and $F_{d\text{-}2}$ are calculated as

$$F_{d-1} = -\frac{3Db^2d\,(1-\cos\delta)}{4(p_2+s)},$$
$$F_{d-2} = 0. \qquad (20)$$

The simultaneous motion of the segments of the leading and trailing dislocations is possible if $F_{1x}>0$ and $F_{2x}>0$. These inequalities can be fulfilled if the value of the applied load σ exceeds some critical stress σ_{c2}. The critical stress σ_{c2} can be found from the conditions $F_{1x}(\sigma=\sigma_{c2})=0$ and $F_{2x}(\sigma=\sigma_{c2})=0$. Substitution of formulae (17)–(20) and the expressions for F_1^{pin}, F_2^{pin}, $F_{1\text{-}2}$, and $F_{2\text{-}1}$ to the latter conditions yields the following system of equations:

$$\sigma_{c2}bd\left(\frac{\sqrt{6}}{6}\sin(2\beta)+\frac{\sqrt{2}}{3}\sin^2\beta\right)$$
$$=\frac{Db^2}{4}\left(8-3\nu+\frac{3d\,(1-\cos\delta)}{p_2+s}\right), \qquad (21)$$

$$Db^2\left(\frac{(1-\nu)d}{2s}+1\right)=$$
$$\frac{2\sqrt{2}}{9}\sin^2\beta\,\sigma_{c2}bd+\gamma d. \qquad (22)$$

Solving the system of equations (21) and (22) for σ_{c2} and s, one can plot the dependences of σ_{c2} on twin thickness d, for various values of p_2. These dependences for the case of nanotwinned Cu, $\beta=\pi/3$ and $\delta=\pi/6$ are depicted in Fig. 7. Fig. 7 demonstrates that the critical stress σ_{c2} decreases with an increase in twin thickness d and/or an increase of the distance p_2 from the trailing dislocation to the GB. Also, the comparison of Figs. 6 and 7 shows that, for a specified twin thickness d, σ_{c2} is always smaller than σ_c^∞. Thus, at $\sigma<\sigma_{c2}$, neither individual dislocation loops nor jogged dislocations should form in columnar-grained nanotwinned metals. At $\sigma_{c2}<\sigma<\sigma_c^\infty$, plastic deformation in such metals should be realized via the emission of jogged dislocations (and, possibly, via the restricted expansion of dislocation loops within individual twins, which, however, do not expand across the whole twins). At $\sigma>\sigma_c^\infty$, the plastic deformation can, in general, be realized both via the formation and motion of jogged dislocations and through the formation and expansion of dislocation loops. However, since the motion of jogged dislocations occurs via the collective motion of their segments in individual twins, it is logical to assume that in the latter case, the expansion of individual dislocation loops should be more kinetically preferable than their collective expansion resulting in the motion of jogged dislocations. In other words, although at $\sigma>\sigma_c^\infty$, both plastic deformation mechanisms can coexist, one can expect that plastic deformation will be realized mainly through the expansion of individual dislocation loops.

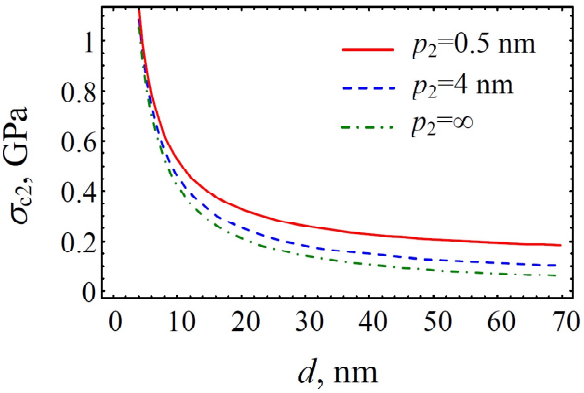

Fig. 7. Dependences of the critical stress σ_{c2} for the motion of a split jogged dislocation on twin thickness d, for various distances p_2 of the trailing dislocation to the grain boundary.

Also, if we fix the applied load σ and vary the twin thickness d, we will get the following scenario for the mechanisms of plastic deformation in columnar-grained nanotwinned metals. At sufficiently small d, such that $\sigma<\sigma_{c2}(d)$ (see Fig. 7), plastic deformation is suppressed. At larger d, such that $\sigma_{c2}(d)<\sigma<\sigma_c^\infty$ (d) (see Figs. 6 and 7), plastic defor-

mation should mainly be realized via the emission of jogged dislocations. At even larger *d*, such that $\sigma > \sigma_c^{\infty}$ (*d*) (see Fig. 6), both plastic deformation mechanisms can coexist, although plastic deformation through the expansion of individual dislocation loops seems to be kinetically easier. This scenario is in accord with the results [25,26] of MD simulations of plastic deformation of columnar-grained nanotwinned Cu loaded parallel to CTBs and nanotwinned multilayered films.

4. CONCLUDING REMARKS

Thus, in this paper we have theoretically analyzed two deformation mechanisms in deformed columnar-grained nanotwinned metals loaded parallel to CTBs. The first mechanism represents the generation of split dislocation loops at GBs and their expansion within individual twins. The second mechanism represents the formation of split jogged dislocations (penetrating multiple twins) at GBs and their motion across the grain interiors. Within our model, both dislocation loops and jogged dislocations nucleate at full pre-existent dislocations located at GBs.

For the case of dislocation loop formation, we have demonstrated that the generation of a leading dislocation loop at a GB is possible even at small applied stresses provided that the Burgers vector of the pre-existent dislocation is favorably oriented. After the generation of the leading dislocation loop, the loop expands until it reaches its equilibrium sizes, followed by the generation and expansion of the trailing dislocation loop. Next, the leading and trailing dislocations expand together as a split dislocation loop. At relatively small applied stresses ($\sigma < \sigma_c^{\infty}$), they reach their equilibrium dimensions while at sufficiently high stresses ($\sigma > \sigma_c^{\infty}$) they expand across the entire twin.

Considering the emission of split jogged dislocations from GBs, we have demonstrated that their formation is possible when the applied load exceeds a critical stress σ_{c2}, and their motion across the grain interior becomes easier as these dislocations move away from the GB. It appeared that for a specified twin thickness *d*, the critical stress σ_{c2} is always smaller than the critical stress σ_c^{∞} for the formation of a split dislocation loop and its expansion across the entire twin. This means that at $\sigma > \sigma_c^{\infty}$, jogged dislocations and dislocation loops expanding across the whole twins can coexist. This result is in contradiction with the previously reported theoretical estimate and MD simulation results [25] suggesting that there should be a critical twin thickness for the transition from one deformation mechanism to another. At the same time, our results are in agreement with the results of MD simulations [26] of Cu/Ag nanotwinned multilayered films with non-uniform layer thickness, where both deformation mechanisms have been observed to act simultaneously.

In conclusion, it should be noted that the present model can be extended to the case of nanotwinned metals with nonuniform twin thickness as well as to nanotwinned metallic alloys. This will be the scope of our future research.

ACKNOWLEDGEMENTS

This work was supported by the Russian Ministry of Education and Science (grant 14.B25.31.0017 and Zadanie 9.1964.2014/K).

REFERENCES

[1] T. Zhu and H. Gao // *Scr. Mater*. **66** (2012) 843.
[2] X. Li and H. Gao, In: *Nano and Cell Mechanics: Fundamentals and Frontiers*, ed. by H.D. Espinosa and G. Bao (Wiley, 2013), p. 129.
[3] I.A. Ovid'ko and A.G. Sheinerman // *Rev. Adv. Mater. Sci.* **44** (2016) 1.
[4] J. Wang and X. Zhang // *MRS Bulletin* **41** (2016) 274.
[5]D.C. Bufford, Y.M. Wang, Y. Liu and L. Lu // *MRS Bulletin* **41** (2016) 286.
[6] F. Sansoz, K. Lu, T. Zhu and A. Misra // *MRS Bulletin* **41** (2016) 292.
[7] X. Li, M. Dao, C. Eberl and A.M. Hodge // *MRS Bulletin* **41** (2016) 298.
[8] N. Li, J. Wang, S. Mao and H. Wang // *MRS Bulletin* **41** (2016) 305.
[9] L. Lu, Y. Shen, X. Chen, L. Qian and K. Lu // *Science* **304** (2004) 422.
[10] L. Lu, X. Chen, X. Huang and K. Lu // *Science* **323** (2009) 607.
[11] K. Lu, L. Lu and S. Suresh // *Science* **324** (2009) 349.
[12] X. Li, Y. Wei, L. Lu, K. Lu and H. Gao // *Nature* **464** (2010) 877.
[13] Y.M. Wang, F. Sansoz, T. LaGrange, R.T. Ott, J. Marian, T.W. Barbee Jr. and A.V. Hamza // *Nature Mater*. **12** (2013) 697.
[14] P. Gu, M. Dao and S. Suresh // *Acta Mater.* **67** (2014) 409.
[15] I.A. Ovid'ko, N.V. Skiba and A.G. Sheinerman // *Rev. Adv. Mater. Sci.* **41** (2015) 93.

[16] I.A. Ovid'ko, N.V. Skiba and A.G. Sheinerman // *Rev. Adv. Mater. Sci*. **43** (2015) 38.
[17] N. Lu, K. Du, L. Lu and H.Q. Ye // *Nat. Commun.* **6** (2015) 7648.
[18] S.V. Bobylev and A.G. Sheinerman // *Rev. Adv. Mater. Sci.* **43** (2015). 31.
[19] R. Yuan, I.J. Beyerlein and C. Zhou // *Acta Mater.* **110** (2016) 8.
[20] I.A. Ovid'ko and A.G. Sheinerman // *Rev. Adv. Mater. Sci*. **47** (2016) 1.
[21] Q. Lu, Z. You, X. Huang, N. Hansen and L. Lu // *Acta Mater.* **127** (2017) 85.
[22] Z.S. You, L. Lu and K. Lu // *Acta Mater.* **59** (2011) 6927.
[23] Z. You, X. Li, L. Gui, Q. Lu, T. Zhu, H. Gao and L. Lu // *Acta Mater.* **61** (2013) 217.
[24] D. Bufford, H. Wang and X. Zhang // *Acta Mater.* **59** (2011) 93.
[25] H. Zhou, X. Li, S. Qu, W. Yang and H. Gao // *Nano Lett.* **14** (2014) 5075.
[26] Y. Zhu, Z. Li, M. Huang and Y. Liu // *Int. J. Plasticity* **72** (2015) 168.
[27] M. Yu. Gutkin and A.G. Sheinerman // *Phys. Status Solidi* B **241** (2004) 1810.
[28] M.Yu. Gutkin and I.A. Ovid'ko // *Phys. Rev.* B **73** (2006) 064102.
[29] J.P. Hirth and J. Lothe, *Theory of Dislocations* (Wiley, New York, 1982).